Viscosity Measurements on Carbon Monoxide, Nitrogen up to 900 Atmospheres and Correlation to Mass Diffusion

GIAN LUIGI CHIERICI

Servizio Geochimico, AGIP-Direzione Mineraria, Milano (Italy)

and ALBERTO PARATELLA

Istituto di Impianti Chimici dell'Universita di Padova (Italy)

At high pressures the viscosity of gaseous mixtures can be measured with great accuracy. For this reason, viscosity data can offer a profitable means of checking other transport properties of the mixture, such as mass diffusivity, which are difficult to measure accurately.

The present paper is aimed to check the experimental mass diffusivity data for the carbon monoxide-nitrogen mixture, which have been obtained by the dynamic method up to 600 atm. (*1, 2*). The application of this method at high pressure is relatively recent; it presents some advantages with respect to the discontinuous method but also some operational difficulties. Thus, a check of the results was needed. To this aim, viscosity measurements have been carried out on the same mixture and the correlation between viscosity and mass diffusivity has been derived by Enskog's theory. The carbon monoxide-nitrogen mixture has been chosen, because the molecular parameters of its components are very similar so that the correlation between the two transport properties approximates that given by Enskog for single gases.

CORRELATION BETWEEN VISCOSITY AND MASS DIFFUSIVITY

In the mixture of components A and B, the binary coefficient of mass diffusion D_{AB}, at pressure P can be expressed by:

$$D_{AB} = (D_{AB})_1 \frac{Z}{P\ X_{AB}} \tag{1}$$

Z is the compressibility factor of the mixture. X_{AB} is a function of P, depending on the diameters of molecules A and B (*3*). $(D_{AB})_1$ denotes the diffusion coefficient calculated at $P = 1$ atm. by the dilute gas theory, at the same temperature of D_{AB}.

In turn, $(D_{AB})_1$ is related to the interaction term, $(\eta_{AB})_1$ (*5*), which appears in the equation for the mixture viscosity, $(\eta_m)_1$:

$$(\eta_m)_1 = (\eta_m)_1\ (\eta_A, \eta_B, \eta_{AB}, x_A, x_B)_1 \tag{2}$$

As in Equation (1), index 1 refers to the state at $P = 1$ atm., $(\eta_A)_1$ and $(\eta_B)_1$ being the viscosities of the single components (*5*) and x_A, x_B the mole fractions.

For the mixture of A = carbon monoxide and B = nitrogen at temperature $T = 323$, 1°K. of our measurements, Equation (2) in the form given by Waldmann (*6*) leads to:

$$\left(\frac{d(\eta_m)_1}{dx_B}\right)_{x_A \to 1} = 1.998\ [(\eta_{AB})_1 - (\eta_A)_1];$$

$$\left(\frac{d(\eta_m)_1}{dx_B}\right)_{x_B \to 1} = 2.000\ [(\eta_B)_1 - (\eta_{AB})_1] \tag{3}$$

Table 1 also shows that $(\eta_A)_1 < (\eta_{AB})_1 < (\eta_B)_1$ and that $(\eta_A)_1 \cong (\eta_B)_1$. According to Equation (3), the interaction term, $(\eta_{AB})_1$, can be simply determined by:

$$(\eta_{AB})_1 \cong \frac{(\eta_A)_1 + (\eta_B)_1}{2} \tag{4}$$

TABLE 1. VISCOSITY VALUES CALCULATED BY THE DILUTE GAS THEORY (*4*)

$P = 1$ atm.; $T = 323.1$°K.	A = CO	B = N_2	CO·N_2
Collision integral (*7*)	0.989	0.998	0.9925
Molecular diameter, Å. (*7*)	3.706	3.681	3.693
Viscosity, 10^6 poise	187.0	187.8	187.6

At high pressures, a correlation of type (2) is no longer available but we find that the linear dependence of η_m on the mixture composition is substantially fulfilled, with $\eta_A \cong \eta_B$. Hence, the term η_{AB} can still be determined from the experimental values η_A, η_B by an equation of type (4), while the calculation can be carried out by an equation which approximates that given by Enskog for the viscosity of single gases (*8*):

$$\eta_i = (\eta_i)_1 \left[\frac{1}{X_i} + 0.800 \left(\frac{b_0}{\overline{V}}\right)_i + 0.761 \left(\frac{b_0}{\overline{V}}\right)_i^2 X_i\right] \qquad i = A;\ B \tag{5}$$

In Equation (5), b_{0i} and $\overline{V}_i$ are the second virial coefficient and the molar volume, respectively, of component i. The term X_i is analogous to X_{AB} of Equation (1).

By putting $i = AB$ in Equation (5), combination of Equations (1) and (5) gives:

$$\eta_{AB} \cong \frac{P}{\alpha\ TZ} \left[D_{AB} + 0.800 \frac{b_0 (D_{AB})_1}{RT} + 0.761 \left(\frac{b_0 (D_{AB})_1}{RT}\right)^2 \frac{1}{D_{AB}}\right] \tag{6}$$

$$\alpha = 3.52 \frac{\Omega_d}{\Omega_v} \tag{7}$$

where Ω_d, Ω_v denote the generalized collision integrals for mass diffusivity and for viscosity, respectively, of the pair AB.

When $P \to 1$, one can recognize in Equation (6) the correlation between viscosity and mass diffusivity as given by Chapman-Enskog (*9*). When P increases, the decreasing of D_{AB} makes the last term in square brackets more and more important until finally it predominates. In this case Equation (6) predicts an inverse proportionality between viscosity and mass diffusivity as for liquids.

In order to apply Equation (6), specification of b_0 is needed. To this aim, we consider the virial coefficients of the components carbon monoxide and nitrogen and we compare them, after checking how the original formulation of such terms is modified at high pressures.

THE INTERMEDIATE AND HIGH PRESSURE REGIONS

Each of these regions corresponds to a different definition of the terms b_{0i} and X_i, which appear in Equations (5) and (6), the limit between the two regions depending upon the particular gas.

In the intermediate region, according to the original definition of X_i:

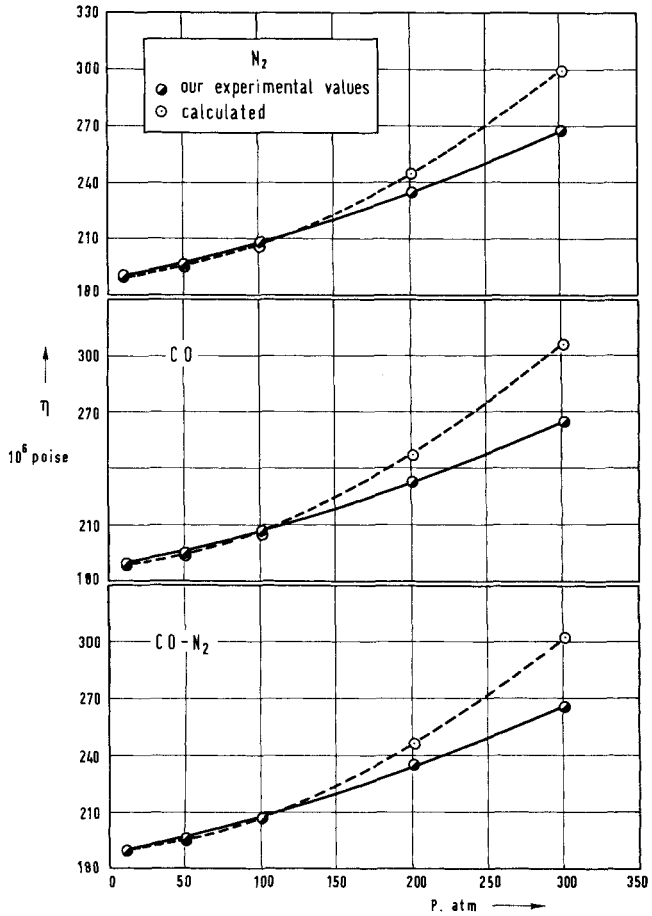

Fig. 1. Comparison between the experimental values of viscosity and those calculated by Equations (5), (9), and (10).

$$X_i = \frac{(P\overline{V}_i/RT) - 1}{(b_0/\overline{V}_i)} \tag{8}$$

the following equations are available (*10*):

$$X_i = 1 + 0.625\left(\frac{b_0}{\overline{V}}\right)_i + 0.2869\left(\frac{b_0}{\overline{V}}\right)_i^2 + 0.115\left(\frac{b_0}{\overline{V}}\right)_i^3 \tag{9}$$

$$\left(\frac{b_0}{\overline{V}}\right)_i = \frac{2}{3}\pi n_i \sigma_i^3 \tag{10}$$

n_i indicates the concentration of molecules i, having diameter σ_i.

By Equations (5), (9), (10) the viscosity of carbon monoxide and nitrogen has been calculated, utilizing the molar volume figures obtained by our P.$\overline{V}$.T. data (see Table 3). Figure 1 shows that the agreement between calculated and experimental values of viscosity is satisfactory only up to 200 atm., as concluded from earlier measurements at 298°K. (*11*).

Table 2. Experimental Viscosities of Carbon Monoxide and of Nitrogen at 50.0°C.

P Int'l. atm.	Viscosity, 10^6 poise CO	N_2	CO·N_2 Equation (*4*)
6	186.7	187.0	186.86
11	188.6	190.3	189.55
51	195.9	196.6	196.1
101	206.4	207.9	207.15
201	232.8	235.7	234.25
301	264.3	267.4	265.35

Beyond 200 atm., which appears to be the upper limit of the intermediate pressure region for both carbon monoxide and nitrogen, Equations (8) and (10) have been modified, substituting pressure P by the total pressure $P_{tot.}$, as given by (*12*):

$$P_{tot.} = T\left(\frac{\partial P}{\partial T}\right)_{\overline{V}} \tag{11}$$

and substituting virial coefficient b_{0i} by the pseudo-virial coefficient b_i, as given by (*12*):

$$b_i = \frac{1}{2.545}\left(\frac{\eta\overline{V}}{(\eta)_1}\right)_{i,\ exp.min.} \tag{12}$$

In Equation (12), $(\eta\overline{V}/(\eta_1)_{i,\ exp.min.}$, indicating the minimum value of the term in brackets for a real gas, must be determined experimentally.

Thus, X_i becomes:

$$X_i = \frac{(\overline{V}_i/R)(\partial P/\partial T)_{\overline{V}_i} - 1}{(b/\overline{V})_i} \tag{13}$$

In order to check the above semiempirical formulae, P.V.T. measurements were carried out in the range from 293 to 373°K. With the experimental values of the compressibility factor, Z, (see Table 3) the slope $(\partial P/\partial T)_{\overline{V}_i} = P/T + (P/Z)(\partial Z/\partial T)_{\overline{V}_i}$ has been graphically determined by the method of residuals (*13*). The term b_i has been obtained from the minimum of the experimental curves reported in Figure 2.

Table 4 shows that the viscosity values calculated by Equations (5), (12), (13) agree with the experimental ones and agreement appears to improve as the pressure increases. In particular, the values of b_i appear to be substantially equal for both carbon monoxide and nitrogen.

Table 4 confirms the reliability of Equations (5), (12), (13) for predicting the viscosity of carbon monoxide and nitrogen and the reliability of Equation (6) for correlating viscosity a mass diffusivity of the carbon monoxide-nitrogen mixture. In Figure 4 the continuous curve collects the val-

Table 3. Compressibility Factor, Z, of Carbon Monoxide and of Nitrogen from Our P.V.T. Measurements

P	CO (Purity 0.9995) Compressibility factor, Z:					N_2 (Purity 0.9999) Compressibility factor, Z:				
int'l. atm.	0°C.	25°C.	50°C.	75°C.	100°C.	0°C.	25°C.	50°C.	75°C.	100°C.
1	1.000	1.000	1.000	1.000	1.000	1.000	1.000	1.000	1.000	1.000
51	0.978	0.991	0.9995	1.006	1.011	0.988	0.999	1.004	1.012	1.016
101	0.972	0.995	1.010	1.021	1.028	0.987	1.007	1.018	1.029	1.036
201	1.019	1.0435	1.062	1.0735	1.082	1.039	1.060	1.077	1.085	1.092
301	1.119	1.133	1.143	1.151	1.155	1.137	1.149	1.159	1.162	1.165
401	1.246	1.245	1.244	1.243	1.241	1.260	1.258	1.257	1.253	1.250
501	1.3825	1.364	1.354	1.342	1.332	1.395	1.3795	1.367	1.3515	1.341
601	1.5225	1.430	1.469	1.448	1.430	1.529	1.499	1.477	1.4535	1.435
701	1.661	1.620	1.585	1.553	1.529	1.665	1.6215	1.590	1.558	1.532
801	1.802	1.747	1.703	1.662	1.628	1.803	1.747	1.7035	1.6625	1.629
901	1.940	1.872	1.816	1.768	1.7265	1.936	1.8695	1.816	1.7675	1.726

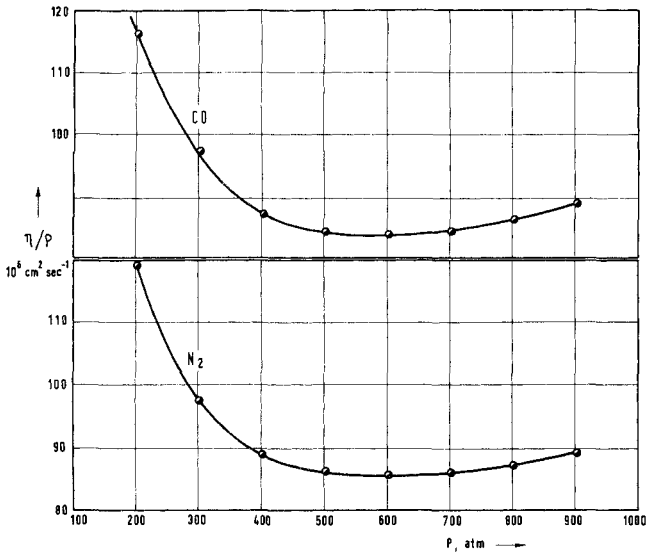

Fig. 2. Experimental values of momentum diffusivity, η/ρ.

Instrument Equation

The instrument equation has been provided because of the difference in construction and operation characteristics between our instrument and other similar devices [that is Eakin's jointed parallelogram device (*14*)].

A preliminary analysis proves the friction losses of laminar flow negligible in comparison to that at the inlet length of the gas capillary which caused by the initial acceleration of the fluid and the change of the velocity profile from a uniform to a parabolic distribution (*15*).

Since the gas capillary and the mercury tube are conical at both ends (cone angle = 1/20), it can be assumed that the entrance and the exit energy losses compensate each other under adiabatic flow conditions.

Thus, neglecting the change in the specific volume of the gas during its displacement, the motion can be described by:

$$\text{mercury} \quad \Delta P = -\rho_{Hg} g h + \frac{8\eta_{Hg} v_{Hg} L_{Hg}}{r^2_{Hg}}$$

TABLE 4. COMPARISON BETWEEN OUR EXPERIMENTAL DATA AND THOSE CALCULATED BY EQUATIONS (5), (12), (13)

	N_2 at 50°C.				CO at 50°C.			
P	$\frac{P_{tot.}\overline{V}_i}{RT} - 1$	$\left(\frac{b}{\overline{V}}\right)_i$	η, 10^6 poise		$\frac{P_{tot.}\overline{V}_i}{RT} - 1$	$\left(\frac{b}{\overline{V}}\right)_i$	η, 10^6 poise	
int'l. atm			calc.	exp.			calc.	exp.
201	0.4644	0.3535	219.6	235.7	0.4265	0.3544	230.0	232.8
301	0.6819	0.4919	257.4	267.4	0.6660	0.4931	258.9	264.3
401	0.8702	0.6044	296.5	300.0	0.8671	0.6034	294.8	296.9
501	1.0382	0.6944	333.0	334.7	1.0451	0.6925	330.5	330.9
601	1.1875	0.7708	368.7	368.8	1.2112	0.7659	364.8	364.3
701	1.3459	0.8350	402.6	401.3	1.3734	0.8278	398.3	399.0
801	1.5008	0.8907	436.3	434.0	1.5287	0.8805	430.9	430.0
901	1.6460	0.9398	469.5	467.7	1.6878	0.9286	464.8	467.4

ues of the binary diffusion coefficient, $D_{CO,\,N_2}$, calculated with Equations (6) and (12) by our viscosity measurements. The circles indicate our experimental values of $D_{CO,\,N_2}$ previously measured at the same temperature by the dynamic method (*2*).

EXPERIMENTAL

Equipment

A viscometer has been built by the Servizio Geochimico, AGIP—Direzione Mineraria, Milano, which satisfactorily compromises accurate measurement and simple operation. Figure 3 shows the main elements: reservoirs a and b, gas capillary c and mercury tube d. These are connected forming a rigid parallelogram, in which mercury and a known quantity of the gas are confined. By automatic control the rigid parallelogram can rotate around point O to assume four inclinations (see Table 5), allowing as many viscosity measurements at the same pressure.

The gas volume forced through the capillary during one run is determined by timing the motion of the mercury level between the two contacts e_1 and e_2.

TABLE 5. CHARACTERISTICS OF THE VISCOMETER. INDEX 0 REFERS TO ZERO VALUE OF THE INCLINATION ANGLE, θ, (SEE FIGURE 3)

$S_0 = 4.909$ sq. cm. $\quad \epsilon_0 = 1.486$ cm. $\quad V = V_0 = 7.295$ cc.

Inclination	$\cos\theta$	$S = S_0/\cos\theta$ sq. cm.	$\epsilon = \epsilon_0 \cos\theta$ cm.	h_1 cm.	h_2 cm.
1	0.9976	4.921	1.482	6.312	3.348
2	0.9934	4.942	1.476	10.464	7.512
3	0.9641	5.092	1.432	24.179	21.315
4	0.9062	5.417	1.347	38.525	35.831

$$\text{gas} \quad -\Delta P = \rho g h + \frac{8\eta v L}{r^2} + \beta\rho v^2 \qquad (14)$$

ΔP denotes the pressure drop corresponding to the height difference, h, (see Figure 3) between the interfaces mercury-gas in reservoirs a and b, ρ and v indicate the density and the mean velocity of the gas through the capillary of length L; ρ_{Hg} and v_{Hg} are the corresponding quantities for the mercury displaced through the tube of length L_{Hg}. The term $\beta\rho v^2$ represents after Langhaar (*16*) the friction loss at the inlet length of the capillary, being β a dimensionless factor which can vary from 1.11 to 1.18 (*17*).

One introduces into Equations (14) the equality between the volume flow rates of the gas and of the mercury:

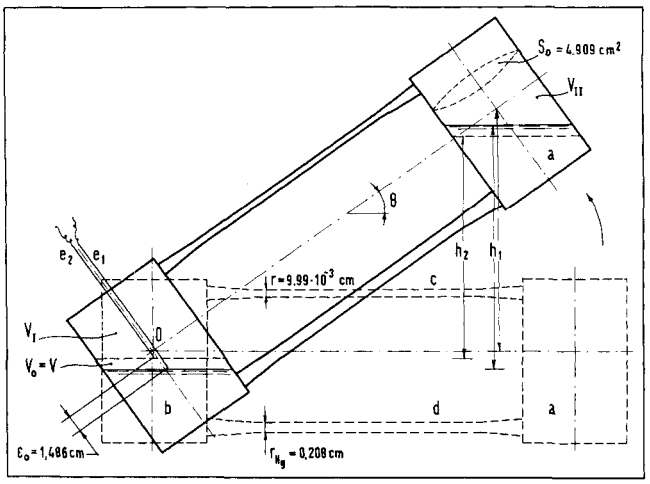

Fig. 3. Layout of the viscometer for measurements up to 1,500 atm.

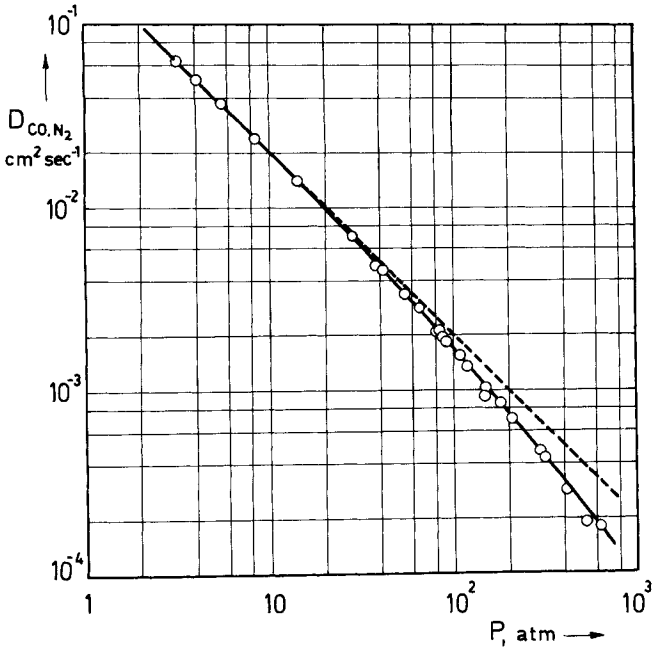

Fig. 4. Mass diffusivity, D_{CO,N_2}, calculated by experimental viscosity data with Equation (6) (continuous curve). The circles refer to experimental mass diffusivity values (2).

$$q = q_{Hg} = -\frac{S}{2}\frac{dh}{dt} \tag{15}$$

with t = time and $S = S_0/\cos\theta$. S is the instantaneous area of the interface mercury-gas (see Figure 3). By combining Equations (14) and (15) we get:

$$a\frac{S^2}{4}\left(\frac{dh}{dt}\right)^2 - \frac{S}{2}(d + d_{Hg})\left(\frac{dh}{dt}\right) - ch = 0 \tag{16}$$

$$a = \frac{\beta\rho}{\pi^2 r^4}; \quad d = \frac{8\eta L}{\pi r^4}; \quad d_{Hg} = \frac{8\eta_{Hg} L_{Hg}}{\pi r^4_{Hg}};$$

$$c = g(\rho_{Hg} - \rho) \tag{17}$$

Under the condition $(dh/dt) < 0$, the solution of Equation (16) is given by the negative root:

$$\frac{dh}{dt} \frac{d + d_{Hg}}{a\ S}\left[1 - (1 + \gamma h)^{1/2}\right] \tag{18}$$

$$\gamma = \frac{4\ a\ c}{(d + d_{Hg})^2} \tag{19}$$

The integral of Equation (18) supplies time $\bar{t}$ required for displacing the gas through the capillary:

$$\bar{t} = \frac{S(d + d_{Hg})}{4\ a}\left\{\ln\frac{h_2}{h_1} + 2[(1 + \gamma h_1)^{1/2} - (1 + \gamma h_2)^{1/2}] + \ln\frac{[(1 + \gamma h_2)^{1/2} + 1]\,[(1 + \gamma h_1)^{1/2} - 1]}{[(1 + \gamma h_2)^{1/2} - 1]\,[(1 + \gamma h_1)^{1/2} + 1]}\right\} \tag{20}$$

h_1 and h_2 being the h values at the beginning and the end of the run, respectively.

In Equation (20) the terms S, d_{Hg}, h_1 and h_2 are known instrument constants. d and γ depend on the viscosity, η. By putting measured time $\bar{t}$, Equation (20) is iteratively solved until a satisfactory value of η is found.

Now, we verify the two main assumptions behind Equation (20). The first is that the gas flow through the capillary is laminar. Equations (14) and (15) have been combined and solved with respect to the gas velocity. This leads to the following expressions for the Reynolds number:

$$N_{Re} = \left[\frac{64\ r^6}{\beta^2}\left(\frac{L}{r^4} + \frac{\eta_{Hg} L_{Hg}}{\eta r^4_{Hg}}\right)^2 + \frac{4\ r^2\ g}{\beta\ \eta^2}\rho h_1(\rho_{Hg} - \rho)\right]^{1/2} - \frac{8r^3}{\beta}\left(\frac{L}{r^4} + \frac{\eta_{Hg} L_{Hg}}{\eta r^4_{Hg}}\right) \tag{21}$$

By Equation (21), the flow appears to be laminar when the instrument operates at the inclination 1 (see Table 5 and Figure 3). For the other inclinations it proved reliable to put into Equation (21) the value of t measured by the instrument at inclination 1 and to verify that the Reynolds number satisfies the condition $N_{Re} \leq 1{,}500$.

The second assumption behind Equation (20) is that the effective displaced volume of gas, V_{eff}, is equal to that $V = \epsilon S$ of mercury. It implies that $\Delta P << P$. To this aim, we consider the instantaneous pressures, P_1^m and P_2^m, in reservoir b at the beginning and at the end of the run:

$$P_1^m = P + gh_1\,(\rho_{Hg} - \rho)\frac{V_{II}}{(V_I + V) + V_{II}};$$

$$P_2^m = P + gh_2\,(\rho_{Hg} - \rho)\frac{V + V_{II}}{(V_I + V) + V_{II}} \tag{22}$$

$(V_I + V)$ and V_{II} indicate the gas volumes at the beginning of the run in reservoirs b and a, respectively. Since the mean pressure is P, the effective displaced volume of gas, V_{eff}, is given by:

$$V_{eff}\,P = (V_I + V)\,P_1^m + V_I\,P_2^m \tag{23}$$

By combining Equations (22) and (23), we get

$$\frac{V_{eff}}{V} = 1 + \frac{\delta}{P} \tag{24}$$

$$\delta = gh_1(\rho_{Hg} - \rho)\ \frac{V_{II}(V_I + V) - V_I\,(V + V_{II})\,(h_2/h_1)}{V(V + V_I + V_{II})} \tag{25}$$

the factor δ varying from 0.1129 atm. at the first inclination to 0.2551 atm. at the last inclination of the instrument. By Equation (25), in the range $P > 50$ atm., the ratio δ/P becomes $\leq 10^{-3}$ and the assumption $V_{eff} \cong V$ is fulfilled. In the range $P \leq 50$ atm., where the above assumption is satisfied only within some units percentage, Equation (20) has been corrected, by substituting the measured time, $\bar{t}$, with time t^* empirically formulated by:

$$t^* = \frac{\bar{t}}{1 + \delta/P} \tag{26}$$

Equation (26) derives from the fact that, when $V_{eff}/V \leq 1.05$, as is the case with $P \leq 50$ atm., the time required for displacing the gas is linearly proportional to the effective displaced volume.

CONCLUSION

In the pressure range up to 900 atm. our viscometer allows viscosity measurements with an accuracy 1%. Within this figure our data on nitrogen agree with those reported by Michels (18).

For the components carbon monoxide and nitrogen at 50°C., Enskog's theory satisfactorily predicts the behavior of the viscosity, whereas beyond 200 atm. is supplemented by P.V.T. measurements. The latter have been carried out with accuracy 1/1,000, which appears to be satisfactory for the present purpose.

The molecular similarity between carbon monoxide and nitrogen enables application of Enskog's theory in order to check the binary mass diffusivity data by those on viscosity.

NOTATION

b_0; b = second virial coefficient for a hard spheres gas and for a real gas, respectively

D_{AB} = binary coefficient of mass diffusion in the mixture of gases A and B
g = gravity acceleration
h = height difference between the interfaces mercury-gas in the viscometer reservoirs
L; L_{Hg} = length of gas capillary and of mercury tube, respectively
n = molecular concentration
N_{Re} = Reynolds number
P; $P_{tot.}$ = experimental and total pressure of the gas, respectively
ΔP = pressure drop corresponding to height difference, h
q; q_{Hg} = volumetric flow rate of the gas and of the mercury, respectively
r; r_{Hg} = radius of gas capillary and of mercury tube, respectively
R = gas law constant
S_0 = area of the interface mercury-gas at zero inclination of the viscometer
S = area of the interface mercury-gas in the viscometer reservoirs during a run
$\bar{t}$; t^* = time required for displacing the mercury and the gas during a run, respectively. $\bar{t} = t^*$ when $P \geq 50$ atm.
T = absolute temperature
X_i = radial distribution function at distance σ_i from the center of a molecule i having diameter σ_i
V = volume between contacts e_1 and e_2 in reservoir b of the viscometer
$V + V_I$ = gas volume in reservoir b of the viscometer at the beginning of the run
V_{II} = gas volume in reservoir a of the viscometer at the beginning of the run
$\overline{V}$ = molar volume
Z = compressibility factor of the gas, $Z = P\overline{V}/RT$

Greek Letters

ϵ_0 = distance between contacts e_1 and e_2 in reservoir b at zero inclination of the viscometer
η; η_{Hg} = viscosity of the gas and of the mercury, respectively
θ = inclination angle of the viscometer
ρ; ρ_{Hg} = density of the gas and of the mercury, respectively
σ_i = molecular diameter of specie i ($i = A, B, AB$)
Ω_d; Ω_v = generalized collision integrals for mass diffusivity and for viscosity of molecular pair AB, respectively
δ = parameter, defined by Equations (24), (25), related to the volume change of the gas during its displacement through the capillary

Subscripts

$( )_1$ = for viscosity and for mass diffusivity at $P = 1$ atm.
i = for component i ($i = A, B, AB$)
1; 2 = for quantities at the beginning and at the end of a run, respectively
eff = for effective displaced volume of gas through the capillary

LITERATURE CITED

1. Paratella, A., Symposium "Dinamica delle Reazioni Chimiche," CSC 5, CNR-Roma, p. 293 (1966).
2. ———, and I. Sorgato, Paper presented at the Fourth Intern. Symposium Catalysis, Novosibirsk (July 1968).
3. Chapman, S., and T. G. Cowling, "The Mathematical Theory of Non-Uniform Gases," 2nd Ed., Chap. 16, Cambridge Univ. Press, Cambridge (1952).
4. Hirschfelder, J. O., C. F. Curtiss, and R. B. Bird, "Molecular Theory of Gases and Liquids," p. 539, John Wiley, New York (1954).
5. *Ibid.*, pp. 528-529.
6. Waldmann, L., in "Handbuch der Physik," S. Flügge, ed., Band 12, Vol. 12, p. 447, Springer Verlag, Berlin (1958).
7. Hirschfelder, J. O., C. F. Curtiss, and R. B. Bird, "Molecular Theory of Gases and Liquids," pp. 1111 and 1127, John Wiley, New York (1954).
8. Chapman, S., and T. G. Cowling, "The Mathematical Theory of Non-Uniform Gases," 2nd Ed., p. 288, Cambridge Univ. Press, England (1952).
9. Kestin, J., Y. Kobayashi, and R. T. Wood, *Physica*, **32**, 1065 (1966).
10. Hirschfelder, J. O., C. F. Curtiss, and R. B. Bird, "Molecular Theory of Gases and Liquids," p. 635, John Wiley, New York (1954).
11. Paratella, A., *Atti Istituto Veneto SS.LL.AA.*, 744, 433 (1966).
12. Hirschfelder, J. O., C. F. Curtiss, and R. B. Bird, "Molecular Theory of Gases and Liquids," pp. 647-657, John Wiley, New York (1954).
13. York, R., *Ind. Eng. Chem.*, **32**, 54 (1949).
14. Eakin, B. R., and R. T. Ellington, *Trans. Am. Inst. Mech. Eng.*, **216**, 85 (1959).
15. Kestin, J., A. B. Cambel, and J. B. Fenn, ed., "Transport properties in gases," p. 27, Northwestern Univ. Press, Evanston, Ill. (1958).
16. Langhaar, H. L., *Trans. Am. Soc. Mech. Eng.*, **A45**, 64 (1942).
17. Swindells, J. F., R. F. Coe, and T. B. Godfrey, *J. Resources*, **48**, 1 (1952).
18. Michels, A., and R. O. Gibson, *Proc. Roy. Soc. (London)*, **A134**, 288 (1931).

Comparison of Lagrangian Time Correlations Obtained from Dispersion Experiments and from Space-Time Correlation Functions

J. M. RODRIGUEZ and G. K. PATTERSON

University of Missouri-Rolla, Rolla, Missouri

The relation between Lagrangian and Eulerian statistics for turbulent flow has been approached only through approximations or models of the actual motion. Some of these approaches have been motivated by a purely theoretical interest in the problem (*1* to 5) and others by need to justify the interpretation of an experimental measurement (*6* to *10*). Altogether, little progress has been made in this endeavor despite its importance in the research on tur-